International Journal of Solids and Structures 48 (2011) 2630–2641

Contents lists available at ScienceDirect

International Journal of Solids and Structures

journal homepage: www.elsevier.com/locate/ijsolstr

The problem of sharp notch in couple-stress elasticity

P.A. Gourgiotis, H.G. Georgiadis *

Mechanics Division, National Technical University of Athens, Zographou GR-15773, Greece

ARTICLE INFO

Article history:
Received 4 March 2011
Received in revised form 11 May 2011
Available online 24 May 2011

Keywords:
Sharp notch
Cracks
Granular media
Microstructure
Micro-mechanics
Couple-stress elasticity
Asymptotic analysis
Boundary layer

ABSTRACT

The problem of sharp notch in couple-stress elasticity is considered in this paper. The problem involves a sharp notch in a body of infinite extent. The body has microstructural properties, which are assumed to be characterized by couple-stress effects. Both symmetric and anti-symmetric loadings at remote regions are considered under plane-strain conditions. The faces of the notch are considered traction free. To determine the field around the tip of the notch, a boundary-layer approach is followed by considering an expansion of the displacements in a form of separated variables in a polar coordinate system. Our analysis is in the spirit of the Knein–Williams and Karp–Karal asymptotic techniques but it is much more involved than its corresponding analysis of standard elasticity due to the complicated boundary value problem (higher-order system of governing PDEs and additional boundary conditions as compared to the standard theory). Eventually, an eigenvalue problem is formulated and this, along with the restriction of a bounded potential energy, provides the asymptotic fields. The cases of a crack and a half-space are analyzed as limit cases of the general notch problem. Certain deviations from the standard classical elasticity results are noted.

1. Introduction

The present work is concerned with the determination of the asymptotic displacement, rotation, strain and stress fields in the vicinity of the tip of a notch within the framework of couple-stress elasticity. This theory assumes that, within an elastic body, the surfaces of each material element are subjected not only to normal and tangential forces but also to moments per unit area. The latter are called *couple-stresses*. Such an assumption is appropriate for materials with granular structure, where the interaction between adjacent elements may introduce internal moments. In this way, characteristic material lengths appear representing the microstructure. As is well-known, the fundamental concepts of the couple-stress theory were first introduced by Voigt (1887) and the Cosserat brothers (1909), but the subject was generalized and reached maturity only in the 1960s with the studies of Toupin (1962), Mindlin and Tiersten (1962), and Koiter (1964).

The theory of couple-stress elasticity assumes that: (i) each material particle has three degrees of freedom, (ii) an augmented form of the Euler–Cauchy principle with a non-vanishing couple traction prevails, and (iii) the strain-energy density depends upon both the strain and the gradient of rotation. The theory is different from the general Cosserat (or micropolar) theory that takes material particles with six independent degrees of freedom (three displacement components and three rotation components, the latter involving rotation of a micro-medium w.r.t. its surrounding medium). Sometimes, the name 'restricted Cosserat theory' appears in the literature for the couple-stress theory.

Couple-stress elasticity had already some successful applications in the 1960s and 1970s mainly on stress-concentration problems concerning holes and inclusions (see e.g. Mindlin, 1963; Weitsman, 1965; Bogy and Sternberg, 1967; Hsu et al., 1972; Takeuti and Noda, 1973; Itou, 1976). In recent years, the couple-stress theory (and related generalized continuum theories) attracted a renewed and growing interest in dealing with problems of microstructured materials. For instance, problems of dislocations, plasticity, fracture and wave propagation have been analyzed within the framework of couple-stress theory. This is due to the inability of the classical theory to predict the experimentally observed size effect and also due to the increasing demand to study problems at very small scales. Work along these lines was done by, among others, Fleck et al. (1994), Vardoulakis and Sulem (1995), Lakes (1995), Huang et al. (1997, 1999), Lubarda and Markenskoff (2000), Bardet and Vardoulakis (2001), Georgiadis and Velgaki (2003), Lubarda (2003), Radi (2007, 2008), and Gourgiotis and Georgiadis (2007, 2008).

For materials with microstructure, the characteristic material length mentioned before may be on the same order as the length of the microstructure. For instance, Chen et al. (1998) developed a continuum model for cellular materials and found that the continuum description of these materials obey a gradient elasticity theory of the couple-stress type. In the latter study, the intrinsic material length was naturally identified with the cell size. Also,

* Corresponding author. Tel.: +30 210 7721365; fax: +30 210 7721302.
E-mail address: georgiad@central.ntua.gr (H.G. Georgiadis).

0020-7683/$ - see front matter © 2011 Elsevier Ltd. All rights reserved.
doi:10.1016/j.ijsolstr.2011.05.010

Chang et al. (2003) associated the microstructural material constants of the couple-stress theory with the particle size and the inter-particle stiffness in a granular material. In addition, couple-stress theory was successfully utilized in the past to model some materials with microstructure like foams (Lakes, 1993) and porous solids (Lakes, 1983). On the other hand, Maranganti and Sharma (2007), employing a technique based on molecular dynamics, showed that gradient effects are unimportant for most crystalline metals and ceramics. Generally, the couple-stress theory is intended to model situations where a material with microstructure is deformed in *very small* volumes, such as in the immediate vicinity of crack tips, notches, small holes and inclusions, and in micrometer indentations. A recent study by Bigoni and Drugan (2007) provides additional references and an interesting account of the determination of couple-stress moduli via homogenization of heterogeneous materials.

Focusing attention now to the notch problem, we should mention that this problem has been extensively studied in the context of classical elasticity since it is a fundamental stress concentration problem (see e.g. Barber, 1992). Asymptotic techniques have mainly been proposed to explore the nature of the solution around the sharp corner of notches. Some of the earlier contributions on the subject were those of Knein (1927), Brahtz (1933), and Williams (1952), treating the plane problem of a sharp notch under various combinations of homogeneous boundary conditions. Other important works on classical elasticity problems of notches and wedges involving distributed tractions and concentrated loads (along the notch faces) are due to Sternberg and Koiter (1958), Karp and Karal (1962), Neuber (1963), Harrington and Ting (1971), Gregory (1979), Leguillon (1988), and Dundurs and Markenscoff (1989). A thorough overview of the subject and an extensive list of references can be found in the review article by Sinclair (2004).

However, there are no analytical or numerical results in the literature regarding the *general* plane-strain problem of a sharp notch (or wedge) in couple-stress elasticity. Indeed, Bogy and Sternberg (1968) studied the particular case of an orthogonal wedge subjected to a distribution of shear tractions only along the one face to show that the indeterminacy of the counterpart problem of classical elasticity does not carry over to the problem treated by couple-stress elasticity (this 'resolution' is due to the fact that the couple-stress theory allows for an asymmetric stress tensor). Also, a few results concern the limit cases of a crack (Sternberg and Muki, 1967; Ejike, 1969; Atkinson and Leppington, 1977; Huang et al., 1997, 1999; Zhang et al., 1998; Grentzelou and Georgiadis, 2005; Gourgiotis and Georgiadis, 2007, 2008; Radi, 2007, 2008), and a half-space (Muki and Sternberg, 1965).

Here, we aim at studying the general plane-strain problem of an atomistically sharp notch in couple-stress elasticity. The problem represents a convenient idealization of certain more practical situations, such as a notch with a very small fillet radius (much smaller than the intrinsic material length in couple-stress elasticity). In general, few notches are likely to be atomistically sharp and the finite radius at the tip of most real notches will lead to only large but finite plastic strains at the apex. However, atomistically sharp notches may occur in fracture of micro-machined silicon structures in the process of wet etching. Indeed, measurements of the notch radius in etched silicon have been reported to be as small as 10 nm (Suwito et al., 1999).

Our analysis is based on the Knein–Williams technique (Knein, 1927; Williams, 1952; Karp and Karal, 1962; Barber, 1992). According to this technique, a set of (r,θ) polar coordinates is attached to the tip of the notch and the displacement field is expanded as an asymptotic series of separated variable terms, each satisfying the field equations and the traction-free boundary conditions on the faces of the notch. This procedure leads to an eigenvalue problem, which, along with the restriction of a bounded potential energy, provides the asymptotic fields. Our results differ in several important respects from the predictions of standard classical elasticity. In particular, our results indicate that: (i) The rotation is always bounded at the vicinity of the tip of the notch. However, the strain field remains singular. (ii) The stress singularity depends not only upon the angle of the notch but also upon the Poisson's ratio ν. (iii) Contrary to the classical case, the strength of the singularity associated with the antisymmetric loading is always stronger than that for the symmetric loading. This finding corroborates the fact that shear effects are more pronounced when couple-stresses are taken into account.

2. Fundamentals of couple-stress elasticity

In this section we recall briefly certain pertinent elements of the theory of couple-stress elasticity. A detailed exposition of the theory can be found in Mindlin and Tiersten (1962) and Koiter (1964). Also, interesting presentations of the theory are contained in the works by Aero and Kuvshinskii (1960), Palmov (1964), and Muki and Sternberg (1965). The basic equations of dynamical couple-stress theory (including the effects of micro-inertia) were given by Georgiadis and Velgaki (2003).

As mentioned before, couple-stress elasticity assumes that: (i) each material particle has three degrees of freedom, (ii) an augmented form of the Euler–Cauchy principle with a non-vanishing couple traction prevails, and (iii) the strain-energy density depends upon both strain and the gradient of rotation.

In the absence of inertia effects, for a control volume CV with bounding surface S, the balance laws for the linear and angular momentum read

$$\int\int_S T_q^{(n)}\,dS + \int\int\int_{CV} F_q\,d(CV) = 0, \tag{1}$$

$$\int\int_S \left(e_{qpk}x_pT_k^{(n)} + M_q^{(n)}\right)dS + \int\int\int_{CV}\left(e_{qpk}x_pF_k + C_q\right)d(CV) = 0, \tag{2}$$

where a Cartesian rectangular coordinate system $Ox_1x_2x_3$ is used along with the indicial notation and the summation convention (the Latin indices span the range (1,2,3)), e_{pqk} is the Levi–Civita alternating symbol, $\mathbf{n}$ is the outward unit vector normal to the surface with direction cosines n_q, $T_p^{(n)}$ is the surface force per unit area, F_p is the body force per unit volume, $M_p^{(n)}$ is the surface moment per unit area, C_p is the body moment per unit volume, and x_q are the components of the position vector of each material particle with elementary volume $d(CV)$.

The pertinent *force-stress* and *couple-stress* tensors are introduced by considering the equilibrium of the elementary material tetrahedron and enforcing (1) and (2), respectively. The force stress tensor σ_{pq} (which is asymmetric) is defined by

$$T_q^{(n)} = \sigma_{pq}n_p \tag{3}$$

and the couple-stress tensor μ_{pq} (which is also asymmetric) by

$$M_q^{(n)} = \mu_{pq}n_p. \tag{4}$$

Moreover, just like the third Newton's law $\mathbf{T^{(n)}} = -\mathbf{T^{(-n)}}$ is proved to hold by considering the equilibrium of a material 'slice', it can also be proved that $\mathbf{M^{(n)}} = -\mathbf{M^{(-n)}}$ (see e.g. Jaunzemis, 1967). The couple-stresses μ_{pq} are expressed in dimensions of [force][length]$^{-1}$. Further, σ_{pq} can be decomposed into a symmetric and anti-symmetric part

$$\sigma_{pq} = \tau_{pq} + \alpha_{pq} \tag{5}$$

with $\tau_{pq} = \tau_{qp}$ and $\alpha_{pq} = -\alpha_{qp}$, whereas it is advantageous to decompose μ_{pq} into its deviatoric $\mu^{(D)}_{pq}$ and spherical $\mu^{(S)}_{pq}$ part in the following manner

$$\mu_{pq} = m_{pq} + \frac{1}{3}\delta_{pq}\mu_{kk}, \tag{6}$$

where $\mu^{(D)}_{pq} \equiv m_{pq}$, $\mu^{(S)}_{pq} \equiv (1/3)\delta_{pq}\mu_{kk}$, and δ_{pq} is the Kronecker delta.

Now, with the above definitions and the help of the Green–Gauss theorem, one may obtain the stress equations of motion. Eq. (2) leads to the following moment equation

$$\partial_p \mu_{pq} + e_{pqk}\sigma_{kp} + C_q = 0, \tag{7}$$

which can also be written as

$$\frac{1}{2}e_{pqk}\partial_l \mu_{lk} + \alpha_{pq} + \frac{1}{2}e_{pqk}C_k = 0, \tag{8}$$

where $\partial_p(\,) \equiv \partial(\,)/\partial x_p$. Note from Eqs. (7) and (8) that the stress tensor σ_{pq} is symmetric in the absence of couple-stresses and body couples.

Further, Eq. (1) leads to the following force equation

$$\partial_p \sigma_{pq} + F_q = 0, \tag{9}$$

or, by virtue of (5), to the equation

$$\partial_p \tau_{pq} + \partial_p \alpha_{pq} + F_q = 0. \tag{10}$$

Moreover, combining (8) and (10) yields the single equation

$$\partial_p \tau_{pq} - \frac{1}{2}e_{pqk}\partial_p\partial_l \mu_{lk} + F_q - \frac{1}{2}e_{pqk}\partial_p C_k = 0. \tag{11}$$

Finally, in view of Eq. (6) and by taking into account that $\mathrm{curl}(\mathrm{div}((1/3)\delta_{pq}\mu_{kk})) = 0$, we write (11) as

$$\partial_p \tau_{pq} - \frac{1}{2}e_{pqk}\partial_p\partial_l m_{lk} + F_q - \frac{1}{2}e_{pqk}\partial_p C_k = 0, \tag{12}$$

which is the final *equation of equilibrium*.

For the kinematical (linear) description of the continuum now, the following quantities are defined

$$\varepsilon_{pq} = \frac{1}{2}(\partial_p u_q + \partial_q u_p), \tag{13}$$

$$\omega_{pq} = \frac{1}{2}(\partial_p u_q - \partial_q u_p), \tag{14}$$

$$\omega_q = \frac{1}{2}e_{pqk}\partial_k u_p, \tag{15}$$

$$\kappa_{pq} = \partial_p \omega_q, \tag{16}$$

where ε_{pq} is the strain tensor, ω_{pq} is the rotation tensor, ω_q is the rotation vector, and κ_{pq} is the curvature tensor (i.e. the gradient of rotation or the curl of the strain) expressed in dimensions of $[\mathrm{length}]^{-1}$. Notice also that Eq. (16) can alternatively be written as

$$\kappa_{pq} = \frac{1}{2}e_{qlk}\partial_p\partial_l u_k = e_{qlk}\partial_l \varepsilon_{pk}. \tag{17}$$

Eq. (17) expresses compatibility for curvature and strain fields. The compatibility equations for the strain components are the usual Saint Venant's compatibility equations (see e.g. Jaunzemis, 1967). Further, the identity $\partial_k\kappa_{pq} = \partial_p\partial_k\omega_q = \partial_p\kappa_{kq}$ defines the compatibility equations for the curvature components. We notice also that $\kappa_{pp} = 0$ because $\kappa_{pp} = \partial_p\omega_p = (1/2)e_{pqk}u_{q,kp} = 0$ and, therefore, κ_{pq} has only eight independent components. The tensor κ_{pq} is obviously an *asymmetric* tensor.

Regarding traction boundary conditions, at any point on a smooth boundary or section, the following three *reduced* force-tractions and two *tangential* couple-tractions should be specified (Mindlin and Tiersten, 1962; Koiter, 1964)

$$P^{(n)}_q = \sigma_{pq}n_p - \frac{1}{2}e_{qpk}n_p\partial_k m_{(nn)}, \tag{18}$$

$$R^{(n)}_q = m_{pq}n_p - m_{(nn)}n_q, \tag{19}$$

where $m_{(nn)} = n_p n_q m_{pq}$ is the normal component of the deviatoric couple-stress tensor m_{pq}. The modifications of the boundary conditions in the case where corners appear along the boundary can be found in Koiter (1964).

It is worth noticing that at first sight, it might seem plausible that the surface tractions (i.e. the force-traction and the couple-traction) can be prescribed arbitrarily on the external surface of the body through relations (3) and (4), which stem from the equilibrium of the material tetrahedron. However, as Koiter (1964) pointed out, the resulting number of six traction boundary conditions (three force-tractions and three couple-tractions) would be in contrast with the *five* geometric boundary conditions that can be imposed. Indeed, since the rotation vector ω_q in couple-stress elasticity is not independent of the displacement vector u_q (as (15) suggests), the normal component of the rotation is fully specified by the distribution of tangential displacements over the boundary. Therefore, only the three displacement and the two tangential rotation components can be prescribed independently. As a consequence, only *five* surface tractions (i.e. the work conjugates of the above five independent kinematical quantities) can be specified at a point of the bounding surface of the body, i.e. Eqs. (18) and (19). On the contrary, in the Cosserat (micropolar) theory, the traction boundary conditions are six since the rotation is fully independent of the displacement vector (see e.g. Nowacki, 1972). In the latter case, the tractions can directly be derived from the equilibrium of the material tetrahedron, so (3) and (4) are the pertinent traction boundary conditions.

Introducing the constitutive equations of the theory is now in order. We assume a linear and isotropic material response, in which case the strain-energy density takes the form

$$\begin{aligned} W &\equiv W(\varepsilon_{pq}, \kappa_{pq}) \\ &= \frac{1}{2}\lambda\varepsilon_{pp}\varepsilon_{qq} + \mu\varepsilon_{pq}\varepsilon_{pq} + 2\eta\kappa_{pq}\kappa_{pq} + 2\eta'\kappa_{pq}\kappa_{qp}, \end{aligned} \tag{20}$$

where $(\lambda, \mu, \eta, \eta')$ are material constants. Then, Eq. (20) leads, through the standard variational manner, to the following constitutive equations

$$\tau_{pq} \equiv \sigma_{(pq)} = \frac{\partial W}{\partial \varepsilon_{pq}} = \lambda\delta_{pq}\varepsilon_{kk} + 2\mu\varepsilon_{pq}, \tag{21}$$

$$m_{pq} = \frac{\partial W}{\partial \kappa_{pq}} = 4\eta\kappa_{pq} + 4\eta'\kappa_{qp}. \tag{22}$$

In view of (21) and (22), the moduli (λ, μ) have the same meaning as the Lamé constants of classical elasticity theory and are expressed in dimensions of $[\mathrm{force}][\mathrm{length}]^{-2}$, whereas the moduli (η, η') account for couple-stress effects and are expressed in dimensions of [force].

Next, incorporating the constitutive relations (21) and (22) into the equation of equilibrium (12) and using the geometric relations (13)–(16), one may obtain the displacement equations of equilibrium (Koiter, 1964)

$$\nabla^2\mathbf{u} - \ell^2\nabla^4\mathbf{u} + \nabla\left[(1-2\nu)^{-1}(\nabla\cdot\mathbf{u}) + \ell^2\nabla^2(\nabla\cdot\mathbf{u})\right] = 0, \tag{23}$$

where ∇^2 is the Laplace operator, ν is Poisson's ratio, $\ell \equiv (\eta/\mu)^{1/2}$ is a characteristic material length, and the absence of body forces and couples is assumed. In the limit $\ell \to 0$, the Navier-Cauchy equations of classical linear isotropic elasticity are recovered from (23).

Indeed, the fact that Eq. (23) have an increased order w.r.t. their limit case (recall that the Navier–Cauchy equations are PDEs of the second order) and the coefficient ℓ multiplies the higher-order term reveals the *singular-perturbation* character of the couple-stress theory and the emergence of associated *boundary-layer* effects. Moreover, applying the gradient and the curl operator to Eq. (23), we obtain the following relations for the dilatation and the rotation, respectively

$$\nabla^2 e = 0, \quad (1-\ell^2\nabla^2)\nabla^2\boldsymbol{\omega} = 0, \tag{24}$$

where $e \equiv \nabla \cdot \mathbf{u}$ is the dilatation (volumetric strain). Thus, we observe that the dilatation is governed by the same equation as in classical elasticity without couple-stresses. We also note that (24a) is of the second order, whereas each Eq. (23) is of the fourth order. As Koiter (1964) pointed out, this fact reconciles the order of the elliptic system (23) with the number of five boundary conditions.

Finally, the following points are of notice: (i) Since $\kappa_{pp} = 0$, $m_{pp} = 0$ is also valid and therefore the tensor m_{pq} has only eight independent components. (ii) The scalar $(1/3)\mu_{kk}$ of the couple-stress tensor does not appear in the final equation of equilibrium, nor in the reduced boundary conditions and the constitutive equations. Consequently, the spherical part of the couple-stress tensor is left indeterminate within the couple-stress theory. (iii) The following restrictions for the material constants should prevail on the basis of a positive definite strain-energy density (Mindlin and Tiersten, 1962)

$$3\lambda + 2\mu > 0, \quad \mu > 0, \quad \eta > 0, \quad -1 < \frac{\eta'}{\eta} < 1. \tag{25}$$

3. The notch under plane strain conditions

A body occupying a domain in the (r,θ)-plane is considered with the z-axis being normal to this plane. All tractions are assumed to act 'inside' the plane and are independent upon z. The following displacement field is then generated

$$u_r \equiv u_r(r,\theta) \neq 0, \quad u_\theta \equiv u_\theta(r,\theta) \neq 0, \quad u_z \equiv 0. \tag{26}$$

It is worth noting that the independence upon the coordinate z of *all* components of the force-stress and couple-stress tensors, under the assumption (26c), was proved by Muki and Sternberg (1965). Indeed, contrary to the respective plane-strain case in the conventional theory, this independence is not obvious within the couple-stress theory. Notice further that except for $\omega_z \equiv \omega$ and $(\kappa_{rz}, \kappa_{\theta z})$ all others components of the rotation vector and the curvature tensor vanish identically in the particular case of plane-strain considered here. Thus, according to Eqs. (13)–(16), we may write

$$\varepsilon_{rr} = \partial_r u_r, \quad \varepsilon_{\theta\theta} = r^{-1}(\partial_\theta u_\theta + u_r), \quad \varepsilon_{r\theta} = (2r)^{-1}(r\partial_r u_\theta - u_\theta + \partial_\theta u_r), \tag{27}$$

$$\omega_z \equiv \omega = (2r)^{-1}(\partial_r(r u_\theta) - \partial_\theta u_r), \quad \kappa_{rz} = \partial_r \omega, \quad \kappa_{\theta z} = r^{-1}\partial_\theta \omega. \tag{28}$$

The non-vanishing components $(\tau_{rr}, \tau_{\theta r}, \tau_{\theta\theta})$ and $(m_{rz}, m_{\theta z})$ follow directly from (21) and (22), respectively. Then, the antisymmetric stresses $(\alpha_{r\theta}, \alpha_{\theta r})$ are found from (8). Vanishing body forces and body couples are assumed in what follows. In view of the above, the following expressions are written

$$\tau_{rr} = (\lambda + 2\mu)\partial_r u_r + \lambda r^{-1}(u_r + \partial_\theta u_\theta), \tag{29a}$$

$$\tau_{\theta\theta} = (\lambda + 2\mu) r^{-1}(u_r + \partial_\theta u_\theta) + \lambda \partial_r u_r, \tag{29b}$$

$$\tau_{r\theta} = \tau_{\theta r} = \mu\big(r^{-1}(\partial_\theta u_r - u_\theta) + \partial_r u_\theta\big), \tag{29c}$$

$$m_{rz} = 4\mu\ell^2 \partial_r \omega, \quad m_{\theta z} = 4\mu\ell^2 r^{-1}\partial_\theta \omega, \tag{30}$$

$$\alpha_{r\theta} = -2\mu\ell^2\nabla^2\omega, \quad \alpha_{\theta r} = -\alpha_{r\theta}, \quad \alpha_{rr} = \alpha_{\theta\theta} = 0. \tag{31}$$

where $\nabla^2(\,) \equiv \partial_r^2(\,) + r^{-1}\partial_r(\,) + r^{-2}\partial_\theta^2(\,)$ is the 2D Laplace operator.

Further, the stresses are provided by (5)

$$\sigma_{rr} = \tau_{rr} = (\lambda + 2\mu)\partial_r u_r + \lambda r^{-1}(u_r + \partial_\theta u_\theta), \tag{32a}$$

$$\sigma_{\theta\theta} = \tau_{\theta\theta} = (\lambda + 2\mu) r^{-1}(u_r + \partial_\theta u_\theta) + \lambda \partial_r u_r, \tag{32b}$$

$$\sigma_{r\theta} = \tau_{r\theta} + \alpha_{r\theta} = \mu\big(r^{-1}(\partial_\theta u_r - u_\theta) + \partial_r u_\theta\big) - 2\mu\ell^2\nabla^2\omega, \tag{32c}$$

$$\sigma_{\theta r} = \tau_{\theta r} + \alpha_{\theta r} = \mu\big(r^{-1}(\partial_\theta u_r - u_\theta) + \partial_r u_\theta\big) + 2\mu\ell^2\nabla^2\omega, \tag{32d}$$

Also, Eq. (24a) now becomes

$$\nabla^2 e = \nabla^2\big(\partial_r u_r + r^{-1}u_r + r^{-1}\partial_\theta u_\theta\big) = 0. \tag{33}$$

Finally, taking into account Eq. (33), the equations of equilibrium in (23) assume the following form

$$b_1 - \ell^2\left[\nabla^2 b_1 - \frac{1}{r^2}b_1 - \frac{2}{r^2}\frac{\partial b_2}{\partial\theta}\right] + \frac{1}{(1-2\nu)}\frac{\partial e}{\partial r} = 0, \tag{34a}$$

$$b_2 - \ell^2\left[\nabla^2 b_2 - \frac{1}{r^2}b_2 + \frac{2}{r^2}\frac{\partial b_1}{\partial\theta}\right] + \frac{1}{(1-2\nu)}\frac{1}{r}\frac{\partial e}{\partial\theta} = 0, \tag{34b}$$

where the quantities b_1 and b_2 are defined as

$$b_1 = \nabla^2 u_r - \frac{1}{r^2}u_r - \frac{2}{r^2}\frac{\partial u_\theta}{\partial\theta}, \tag{35a}$$

$$b_2 = \nabla^2 u_\theta - \frac{1}{r^2}u_\theta + \frac{2}{r^2}\frac{\partial u_r}{\partial\theta}. \tag{35b}$$

Our aim now is to determine the displacement and stress fields near the apex of the notch. Here we deal with the idealized problem of an atomistically sharp notch, where it is assumed that the notch radius is much smaller than the intrinsic material length ℓ in couple-stress elasticity. We focus our attention on the immediate vicinity of the corner and consider, thus, the notch under remotely applied plane loading. The faces of the notch are taken along the planes $\theta = \pm\alpha$ ($\mathbf{n} = \pm\mathbf{e}_\theta$) and are assumed to be traction-free (Fig. 1).

In analogy with the asymptotic method of Knein (1927), Williams (1952), and Karp and Karal (1962), we assume that for sufficiently small r the leading terms of the displacement components may be represented in the following separated variable form

$$\begin{aligned} u_r(r,\theta) &= r^p U_0(\theta) + r^{p+2}U_1(\theta), \\ u_\theta(r,\theta) &= r^p V_0(\theta) + r^{p+2}V_1(\theta), \end{aligned} \tag{36}$$

where p is (in general) a complex constant and $(U_b(\theta), V_b(\theta))$ with $(b = 1,2)$ are angular functions to be determined.

It should be noticed that for the notch problem, a displacement based formulation is more advantageous than a direct stress formulation, since, as we shall have occasion to see shortly, the singularities of the stress and couple-stress fields vary differently with respect to the angle of the notch. Moreover, we note that due to the singular perturbation character of the constitutive Eqs. (32c,d) and the field Eqs. (34), the higher order terms $\sim r^{p+2}$ must also be taken into account in the displacement asymptotic expansion. In particular, contrary to the classical elasticity case, the form of the normal and shear stresses is different in couple-stress elasticity. Indeed, according to Eqs. (32), it is readily seen that the normal stresses depend only on the first gradient of displacement, while the shear stresses depend on both the first and the third gradient of displacement. Therefore, as will become apparent later in this section, these higher order terms are coupled with the dominant terms $\sim r^p$, to satisfy the boundary condition of vanishing

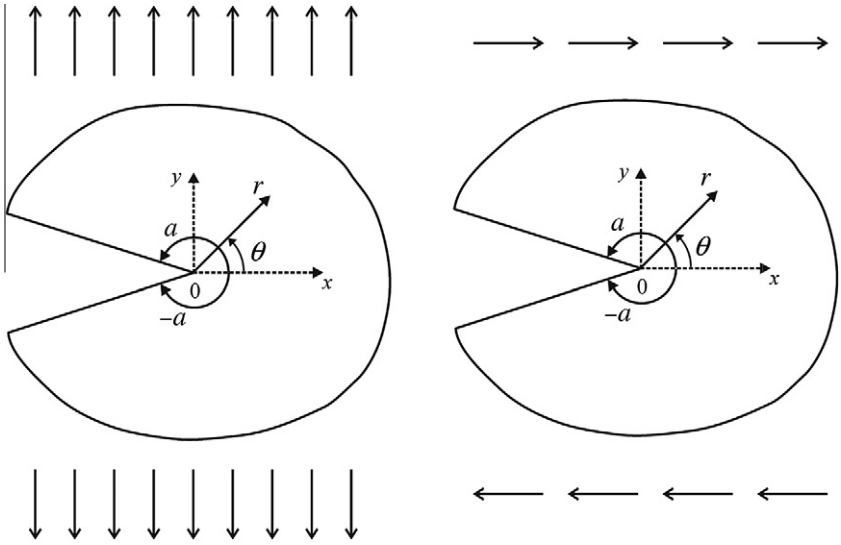

Fig. 1. Geometry of the elastic notch under plane-strain conditions: (a) Symmetric loading (b) Antisymmetric loading.

shear stresses at the faces of the notch. Neglecting these terms leads to the erroneous conclusion that the antisymmetric part of the stress field α_{pq} has no contribution to the *dominant* part of the (asymmetric) stress field σ_{pq}. This, in turn, would imply that the stress tensor is symmetric in the vicinity of the notch tip. However, this finding is in contrast with previous results concerning the limit case of a crack (Sternberg and Muki, 1967; Huang et al., 1997; Gourgiotis and Georgiadis, 2007, 2008), where it was shown that the antisymmetric part of the stress tensor is not zero, and thus the stress tensor is asymmetric at the crack-tip. The particular form of expansion in (36) is therefore necessary, in our boundary layer analyses, towards the understanding of the structure of the near-tip fields. Finally, it is worth noting that in dipolar gradient elasticity considering these higher-order terms is not necessary in the asymptotic solution of the respective notch problem due to the nature of the field equations and the boundary conditions of the theory (Gourgiotis et al., 2010).

Now, (33) and (34) are the governing equations of our problem. Substituting Eq. (36) in the field Eqs. (34) and equating coefficients of like powers of r, we obtain the following homogeneous coupled system of ordinary differential equations for the angular functions $U_0(\theta)$ and $V_0(\theta)$:

$$\begin{cases} U_0^{iv} + 2(p^2-2p-1)U_0'' + (p-1)^2(p-3)(p+1)U_0 \\ \quad -4V_0''' - 4(p-1)^2V_0' = 0, \\ V_0^{iv} + 2(p^2-2p-1)V_0'' + (p-1)^2(p-3)(p+1)V_0 \\ \quad +4U_0''' + 4(p-1)^2U_0' = 0, \end{cases} \tag{37}$$

where primes denote differentiation with respect to θ.

The homogeneous system (37) admits the following general solution:

$$U_0(\theta) = A_1\cos(p-1)\theta + A_2\cos(p+1)\theta + A_4\cos(p-3)\theta + B_1\sin(p-1)\theta + B_2\sin(p+1)\theta + B_4\sin(p-3)\theta, \tag{38a}$$

$$V_0(\theta) = -A_1\frac{(p-1)}{p+1}\sin(p-1)\theta - A_2\sin(p+1)\theta + A_3\sin(p-1)\theta + A_4\sin(p-3)\theta + B_1\frac{(p-1)}{p+1}\cos(p-1)\theta + B_2\cos(p+1)\theta + B_3\cos(p-1)\theta - B_4\cos(p-3)\theta, \tag{38b}$$

where the unknown constants A_b and B_b (with $b = 1,2,3,4$) correspond to symmetric and antisymmetric loadings, respectively. Moreover, according to the above procedure, the angular functions $U_1(\theta)$ and $V_1(\theta)$ are determined from the solution of a system of non-homogeneous differential equations given in Appendix A. Finally, it is noted that the solution in (38) should also satisfy Eq. (33), which, in turn, implies that $A_4 = B_4 = 0$ (see Appendix A).

In light of the above, the displacement field takes the following form

Symmetric loading

$$u_r = r^p\{A_1\cos(p-1)\theta + A_2\cos(p+1)\theta\} + r^{p+2}\left\{\frac{(p-1)}{4(1-2\nu)\ell^2(p+1)}\left[\frac{(1-\nu)}{(p+1)}A_1 + \frac{(p-3+4\nu)}{8p}A_3\right] \times \cos(p-1)\theta + C_1\cos(p+1)\theta - C_2\cos(p+3)\theta\right\}, \tag{39a}$$

$$u_\theta = r^p\left\{-A_1\frac{(p-1)}{p+1}\sin(p-1)\theta - A_2\sin(p+1)\theta + A_3\sin(p-1)\theta\right\} + r^{p+2}\left\{-\frac{(p+3)}{4(1-2\nu)\ell^2(p+1)}\left[\frac{(1-\nu)}{(p+1)}A_1 + \frac{(p-3+4\nu)}{8p}A_3\right] \times \sin(p-1)\theta + C_2\sin(p+3)\theta + C_3\sin(p+1)\theta\right\}. \tag{39b}$$

Antisymmetric loading

$$u_r = r^p\{B_1\sin(p-1)\theta + B_2\sin(p+1)\theta\} + r^{p+2}\left\{\frac{(p-1)}{4(1-2\nu)\ell^2(p+1)}\left[\frac{(1-\nu)}{(p+1)}B_1 - \frac{(p-3+4\nu)}{8p}B_3\right] \times \sin(p-1)\theta + D_1\sin(p+1)\theta + D_2\sin(p+3)\theta\right\}, \tag{40a}$$

$$u_\theta = r^p\left\{B_1\frac{(p-1)}{p+1}\cos(p-1)\theta + B_2\cos(p+1)\theta + B_3\cos(p-1)\theta\right\} + r^{p+2}\left\{\frac{(p+3)}{4(1-2\nu)\ell^2(p+1)}\left[\frac{(1-\nu)}{(p+1)}B_1 - \frac{(p-3+4\nu)}{8p}B_3\right] \times \cos(p-1)\theta + D_2\cos(p+3)\theta + D_3\cos(p+1)\theta\right\}, \tag{40b}$$

where (C_b, D_b) with $(b = 1,2,3)$ are unknown constants corresponding to symmetric and antisymmetric loadings, respectively.

Further, according to Eqs. (27) and (28), the dominant asymptotic fields for the strain, rotation and curvature become

$$\varepsilon_{rr} = r^{p-1}p\{A_1\cos(p-1)\theta + A_2\cos(p+1)\theta\} + r^{p-1}p\{B_1\sin(p-1)\theta + B_2\sin(p+1)\theta\} + O(r^{p+1}), \tag{41a}$$

$$\varepsilon_{\theta\theta} = r^{p-1}\left\{-A_1\frac{p(p-3)}{(p+1)}\cos(p-1)\theta - A_2p\cos(p+1)\theta + A_3(p-1)\cos(p-1)\theta\right\} - r^{p-1}\left\{B_1\frac{p(p-3)}{(p+1)}\sin(p-1)\theta + B_2p\sin(p+1)\theta + B_3(p-1)\sin(p-1)\theta\right\} + O(r^{p+1}), \tag{41b}$$

$$\varepsilon_{r\theta} = r^{p-1}\left\{-A_1\frac{p(p-1)}{(p+1)}\sin(p-1)\theta - A_2p\sin(p+1)\theta + A_3\frac{(p-1)}{2}\sin(p-1)\theta\right\} + r^{p-1}\left\{B_1\frac{p(p-1)}{(p+1)}\cos(p-1)\theta + B_2p\cos(p+1)\theta + B_3\frac{(p-1)}{2}\cos(p-1)\theta\right\} + O(r^{p+1}), \tag{41c}$$

$$\omega = \frac{1}{2}r^{p-1}A_3(p+1)\sin(p-1)\theta + \frac{1}{2}r^{p-1}B_3(p+1)\cos(p-1)\theta + O(r^{p+1}), \tag{42}$$

$$\kappa_{rz} = \frac{1}{2}r^{p-2}A_3(p^2-1)\sin(p-1)\theta + \frac{1}{2}r^{p-2}B_3(p^2-1)\cos(p-1)\theta + O(r^p), \tag{43a}$$

$$\kappa_{\theta z} = \frac{1}{2}r^{p-2}A_3(p^2-1)\cos(p-1)\theta - \frac{1}{2}r^{p-2}B_3(p^2-1)\sin(p-1)\theta + O(r^p). \tag{43b}$$

Similarly, (29)–(32) provide the dominant asymptotic fields for the stress and couple stress components

$$\tau_{\theta r} = \tau_{r\theta} = -\mu r^{p-1}\left\{A_1\frac{2p(p-1)}{(p+1)}\sin(p-1)\theta + 2A_2p\sin(p+1)\theta - A_3(p-1)\sin(p-1)\theta\right\} + \mu r^{p-1}\left\{B_1\frac{2p(p-1)}{(p+1)}\cos(p-1)\theta + 2B_2p\cos(p+1)\theta + B_3(p-1)\cos(p-1)\theta\right\} + O(r^{p+1}), \tag{44}$$

$$\alpha_{r\theta} = -\alpha_{\theta r} = \frac{\mu}{(1-2\nu)}r^{p-1}\left\{A_1\frac{8p(1-\nu)}{(p+1)}\sin(p-1)\theta + A_3(p+4\nu-3)\sin(p-1)\theta\right\} - \frac{\mu}{(1-2\nu)}r^{p-1}\left\{B_1\frac{8p(1-\nu)}{(p+1)}\cos(p-1)\theta - B_3(p+4\nu-3)\cos(p-1)\theta\right\} + O(r^{p+1}), \tag{45}$$

$$\sigma_{rr} = \tau_{rr} = \frac{2\mu}{(1-2\nu)}r^{p-1}\left\{-A_1\frac{p(2p\nu-p-2\nu-1)}{(p+1)}\cos(p-1)\theta + A_2(1-2\nu)p\cos(p+1)\theta + A_3\nu(p-1)\cos(p-1)\theta\right\} - \frac{2\mu}{(1-2\nu)}r^{p-1}\left\{B_1\frac{p(2p\nu-p-2\nu-1)}{(p+1)}\sin(p-1)\theta - B_2(1-2\nu)p\sin(p+1)\theta + B_3\nu(p-1)\sin(p-1)\theta\right\} + O(r^{p+1}), \tag{46a}$$

$$\sigma_{\theta\theta} = \tau_{\theta\theta} = \frac{2\mu}{(1-2\nu)}r^{p-1}\left\{A_1\frac{p(2p\nu-p-2\nu+3)}{(p+1)}\cos(p-1)\theta - A_2(1-2\nu)p\cos(p+1)\theta + A_3(1-\nu)(p-1)\cos(p-1)\theta\right\} + \frac{2\mu}{(1-2\nu)}r^{p-1}\left\{B_1\frac{p(2p\nu-p-2\nu+3)}{(p+1)}\sin(p-1)\theta - B_2(1-2\nu)p\sin(p+1)\theta - B_3(1-\nu)(p-1)\sin(p-1)\theta\right\} + O(r^{p+1}), \tag{46b}$$

$$\sigma_{r\theta} = \tau_{r\theta} + \alpha_{r\theta} = \frac{2\mu}{(1-2\nu)}r^{p-1}\left\{A_1\frac{p(2p\nu-p+5-6\nu)}{(p+1)}\sin(p-1)\theta - A_2(1-2\nu)p\sin(p+1)\theta - A_3(p\nu-p+2-3\nu)\sin(p-1)\theta\right\} - \frac{2\mu}{(1-2\nu)}r^{p-1}\left\{B_1\frac{p(2p\nu-p+5-6\nu)}{(p+1)}\cos(p-1)\theta - B_2(1-2\nu)p\cos(p+1)\theta + B_3(p\nu-p+2-3\nu)\cos(p-1)\theta\right\} + O(r^{p+1}), \tag{46c}$$

$$\sigma_{\theta r} = \tau_{\theta r} + \alpha_{\theta r} = \frac{2\mu}{(1-2\nu)}r^{p-1}\left\{A_1\frac{p(2p\nu-p-3+2\nu)}{(p+1)}\sin(p-1)\theta - A_2(1-2\nu)p\sin(p+1)\theta - A_3(p\nu+\nu-1)\sin(p-1)\theta\right\} - \frac{2\mu}{(1-2\nu)}r^{p-1}\left\{B_1\frac{p(2p\nu-p-3+2\nu)}{(p+1)}\cos(p-1)\theta - B_2(1-2\nu)p\cos(p+1)\theta + B_3(p\nu+\nu-1)\cos(p-1)\theta\right\} + O(r^{p+1}), \tag{46d}$$

$$m_{rz} = 2\mu\ell^2r^{p-2}A_3(p^2-1)\sin(p-1)\theta + 2\mu\ell^2r^{p-2}B_3(p^2-1)\times\cos(p-1)\theta + O(r^p), \tag{47a}$$

$$m_{\theta z} = 2\mu\ell^2r^{p-2}A_3(p^2-1)\cos(p-1)\theta - 2\mu\ell^2r^{p-2}B_3(p^2-1)\times\sin(p-1)\theta + O(r^p). \tag{47b}$$

On examining the previous asymptotic solution, one observes that the antisymmetric part of stress $\alpha_{r\theta}$ exhibits an r^{p-1} behavior. However, the fact that both $\tau_{r\theta}$ and $\alpha_{r\theta}$ have singularities of equal order is surprising in view of Eqs. (31) and (36): evidently, the higher-order singularities in $\alpha_{r\theta}$ generated through the differentiation of the dominant part of the displacement field r^p cancel out. Indeed, it can be readily shown that the dominant part of the displacement field satisfies the equation: $\nabla^2\omega = 0$. Thus, according to (31), *only* the higher-order terms ($\sim r^{p+2}$) in the displacement field contribute to the antisymmetric part of the stress tensor. As a consequence, both the symmetric and the antisymmetric part of stress behave as r^{p-1} in the vicinity of the apex of the notch (see Eqs. (44) and (45)). If this were not the case, the shear stresses (46c,d) would have been more singular than the normal stresses (46a,b), a result that is physically inadmissible for the notch problem. It is further noted that if the higher order terms, in the asymptotic expansion of the displacement field, were not taken into account the antisymmetric part of the stress field would have no contribution to the dominant part of the (asymmetric) stress field σ_{pq}.

Next, the strain energy density becomes

$$W = W_{\text{strain}} + W_{\text{curv.}} = \left[(\lambda/2)(\varepsilon_{rr}+\varepsilon_{\theta\theta})^2 + \mu(\varepsilon_{rr}^2 + 2\varepsilon_{r\theta}^2 + \varepsilon_{\theta\theta}^2)\right] + \left[2\mu\ell^2(\kappa_{rz}^2 + \kappa_{\theta z}^2)\right], \tag{48}$$

where W_{strain} is the part of the strain-energy density due to strains and $W_{\text{curv.}}$ is the part due to curvatures. Substituting Eqs. (41) and (43) into (48) we obtain

$$W_{\text{strain}} = \mu r^{2p-2}f(p,\theta), \tag{49}$$

$$W_{\text{curv.}} = \frac{1}{2}\mu\ell^2r^{2p-4}(p^2-1)^2[A_3^2 + B_3^2], \tag{50}$$

where $f(p,\theta)$ is a function of the exponent p and the angular coordinate θ. It is noted that $W_{\text{curv.}}$ depends only upon the amplitudes A_3 and B_3.

In our analysis we consider the body under remotely applied loading, without any concentrated load applied inside the body or on the boundary. Therefore, the total strain-energy U in a small region surrounding the notch apex (as $r \to 0$) should vanish. It can

further be checked that the total strain-energy per unit length (along the z-axis) in a small circular area around the tip of the notch is given by $U=\int_{-a}^{a}\int_{0}^{r_0} W r\,dr\,d\theta$ (Barber, 1992). The above requirements impose, according to (49) and (50), the following restrictions on the exponent p:

$$p>1 \quad \text{if} \quad \boldsymbol{\kappa}\neq 0 \quad \text{and} \quad p>0 \quad \text{if} \quad \kappa=0. \tag{51}$$

The case $\boldsymbol{\kappa}=0$ necessarily implies that $W_{\text{curv.}}=0$, and occurs either when $p=1$ or when $A_3=B_3=0$.

The boundary conditions for a traction-free notch at $\theta=\pm a$ read

$$\sigma_{\theta\theta}(r,\pm a)=0, \quad \sigma_{\theta r}(r,\pm a)=0, \quad m_{\theta z}(r,\pm a)=0. \tag{52}$$

In view of the above, the homogeneous system (52) takes the following form for the symmetric loading case

$$\begin{bmatrix} p(2p\nu-p-2\nu+3)\cos(p-1)a & -(1-2\nu)p(p+1)\cos(p+1)a & (1-\nu)(p^2-1)\cos(p-1)a \\ p(2p\nu-p+2\nu-3)\sin(p-1)a & -(1-2\nu)p(p+1)\sin(p+1)a & -(p\nu-1+\nu)(p+1)\sin(p-1)a \\ 0 & 0 & (p^2-1)\cos(p-1)a \end{bmatrix}\begin{bmatrix} A_1 \\ A_2 \\ A_3 \end{bmatrix}=0, \tag{53}$$

whereas for antisymmetric loading becomes

$$\begin{bmatrix} p(2p\nu-p-2\nu+3)\sin(p-1)a & -(1-2\nu)p(p+1)\sin(p+1)a & -(1-\nu)(p^2-1)\sin(p-1)a \\ p(2p\nu-p+2\nu-3)\cos(p-1)a & -(1-2\nu)p(p+1)\cos(p+1)a & (p+1)(p\nu+\nu-1)\cos(p-1)a \\ 0 & 0 & (p^2-1)\sin(p-1)a \end{bmatrix}\begin{bmatrix} B_1 \\ B_2 \\ B_3 \end{bmatrix}=0. \tag{54}$$

We note that the first two elements of the last row in the above matrices are zero. This is due to the fact that the dominant part of the rotation in (42) and consequently the dominant part of couple stresses in (47), does not depend upon the amplitudes (A_1,A_2) and (B_1,B_2), respectively.

Now, for the existence of a non-trivial solution, the determinants of the coefficients of (A_b,B_b) should vanish and this gives the following characteristic equations for p:

Symmetric loading

$$a_{33}^{(s)}\cdot M_{33}^{(s)}=\left[(p^2-1)\cos(p-1)a\right]\cdot\left[(1-2\nu)p\sin 2a-(3-2\nu)\sin 2ap\right]=0, \tag{55}$$

Antisymmetric loading

$$a_{33}^{(a)}\cdot M_{33}^{(a)}=\left[(p^2-1)\sin(p-1)a\right]\cdot\left[(1-2\nu)p\sin 2a+(3-2\nu)\sin 2ap\right]=0, \tag{56}$$

where $M_{33}^{(s)}$ and $M_{33}^{(a)}$ are the minor determinants of the elements $a_{33}^{(s)}$ and $a_{33}^{(a)}$ in the matrices (53) and (54), respectively. It is apparent that the eigenvalue $p=1$ satisfies the characteristic equations for all notch angles. The case $p=1$ requires separate treatment because the differential equations in (37) become degenerate, and thus admit a special solution. However, by enforcing the boundary conditions (52) in conjunction with Eq. (33), it can be shown that this special solution coincides with our general solution in (38) for $p=1$. The displacement field associated with this eigenvalue results to a constant strain field, and also it does not produce couple stresses (note, that in this case $\boldsymbol{\kappa}=0$). Therefore, according to (51b), $p=1$ is a physically admissible eigenvalue since it leads, for all angles a, to bounded potential energy.

The following cases are now considered for the symmetric and antisymmetric loadings:

Symmetric loading

S1. $M_{33}^{(s)}=0$ and $a_{33}^{(s)}\neq 0$,

S2. $M_{33}^{(s)}\neq 0$ and $a_{33}^{(s)}=0$.

Antisymmetric loading

A1. $M_{33}^{(a)}=0$ and $a_{33}^{(a)}\neq 0$,

A2. $M_{33}^{(a)}\neq 0$ and $a_{33}^{(a)}=0$.

Fig. 2 depicts the locus of roots of the characteristic Eq. (55). The solid and dotted lines are the roots of the minor determinant $M_{33}^{(s)}$ for Poisson's ratios $\nu=0$ and $\nu=0.5$, respectively. The dashed-dot lines correspond to the roots of the equation $a_{33}^{(s)}=0$. It is observed that for notch angles $90^\circ<a<180^\circ$ the two transcendental equations: $M_{33}^{(s)}=0$ and $a_{33}^{(s)}=0$, share no common roots. In this range, the singularity of the stress field is deduced from equation $M_{33}^{(s)}=0$, whereas the singularity of the couple-stress field is determined by $a_{33}^{(s)}=0$. Indeed, it can readily be shown that in S1 case the satisfaction of the boundary conditions in (52) necessarily implies that $A_3=0$. Therefore, according to (42) and (47), the dominant part of the displacement field is *irrotational* and it does not produce couple-stresses. Moreover, in this case, we also have $W_{curv.}=0$ and thus $p>0$. In light of the above, we conclude that

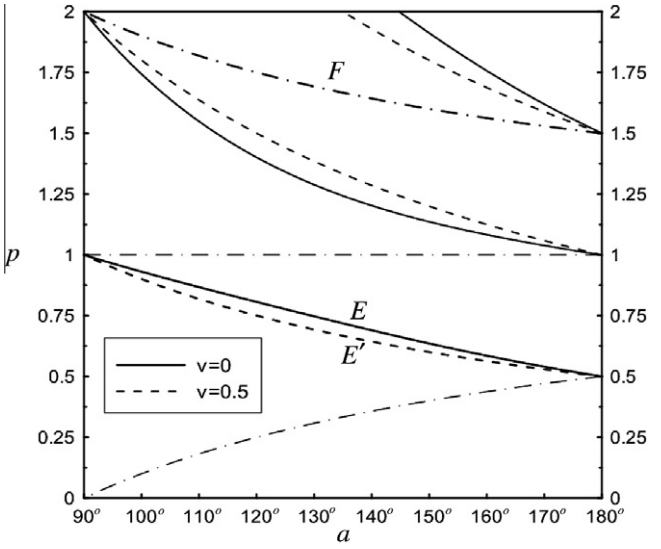

Fig. 2. Locus of roots: Symmetric loading. Solid ($\nu=0$) and dotted ($\nu=0.5$) lines represent the roots of $M_{33}^{(s)}$. Dash–dot lines represent the roots of $a_{33}^{(s)}$.

the variation of the stress singularity will be given from curves E ($\nu = 0$) and E' ($\nu = 0.5$) in Fig. 2. On the other hand, in S2 case we necessarily have $A_3 \neq 0$. In addition, the satisfaction of the boundary conditions in (52) yields: $A_2 = 0$ and $A_1 = f(A_3)$. Accordingly, the displacement field gives rise to couple stresses and therefore $W_{\text{curv.}} \neq 0$. In this case, the exponent p must satisfy the inequality: $p > 1$. Hence, the singularity of the couple stress field is determined from curve F in Fig. 2.

Finally, we note that at points $\alpha = 180°$ (crack) and $\alpha = 90°$ (half-space), $M_{33}^{(s)}$ and $a_{33}^{(s)}$ have common roots (see Fig. 2). In particular, in the mode I crack case, the first common root is $p = 1/2$. In this case, the satisfaction of the boundary conditions in (52) along with the requirement of bounded potential energy at the tip of the notch, indicate that $A_3 = 0$. Thus, the dominant displacement field in the mode I crack problem is irrotational (Huang et al., 1997). The second common eigenvalue is $p = 1$. This eigenvalue is associated with a constant stress field and does not produce couple-stresses. In light of the above, we gather that the eigenvalue $p = 1/2$ characterizes the dominant singularity of the stress field, whereas $p = 3/2$ (which is the third common eigenvalue) the dominant singularity of the couple stress field.

Similar results apply in the antisymmetric loading case. Fig. 3 displays the roots of the characteristic Eq. (56). Again, in the range $90° < \alpha < 180°$, the two transcendental equations $M_{33}^{(a)} = 0$ and $a_{33}^{(a)} = 0$, have no common roots. In this range, the singularity of the stress field is defined by $M_{33}^{(a)} = 0$, while the singularity of the couple-stress field is determined by $a_{33}^{(a)} = 0$. Indeed, in the case A1, the boundary conditions (52) furnish $B_3 = 0$. Thus, according to (42), (43) and (47), the dominant part of the rotation, curvature and couple stress field is zero. Moreover, in this case we have $p > 0$, and therefore the variation of the singularity of the stress field is given by curves G and G' (Fig. 3). In A2 case we have $B_3 \neq 0$. Consequently, the exponent p must satisfy the inequality: $p > 1$. The first curve that meets the above requirements is H (Fig. 3), which, in turn, defines the singularity of the couple stress field. Finally, by arguments similar to those used in the symmetric case, it is readily shown that in the mode II crack problem the dominant stress and couple stress singularities are associated with the eigenvalues $p = 1/2$ and $p = 2$, respectively.

In Fig. 4, the variation of the stress singularity $(p - 1)$ is displayed. It is observed that as the angle of the notch decreases from 180° to 90°, the strength of the singularity falls monotonically from

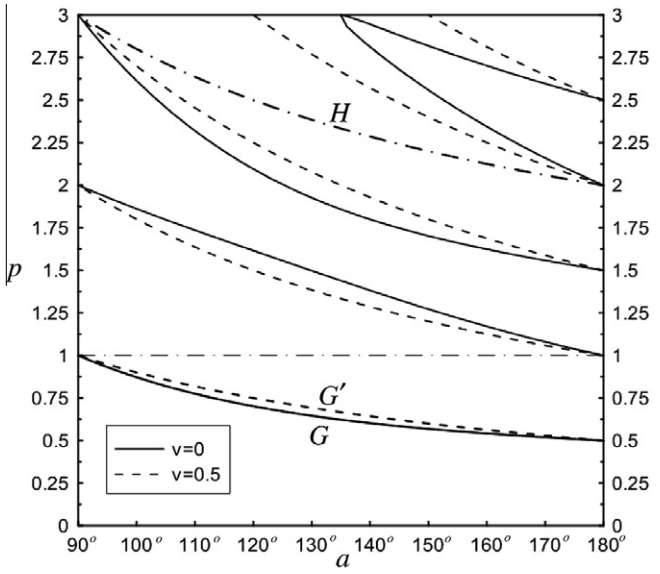

Fig. 3. Locus of roots: Antisymmetric loading. Solid ($\nu = 0$) and dotted ($\nu = 0.5$) lines represent the roots of $M_{33}^{(a)}$. Dash–dot lines represent the roots of $a_{33}^{(a)}$.

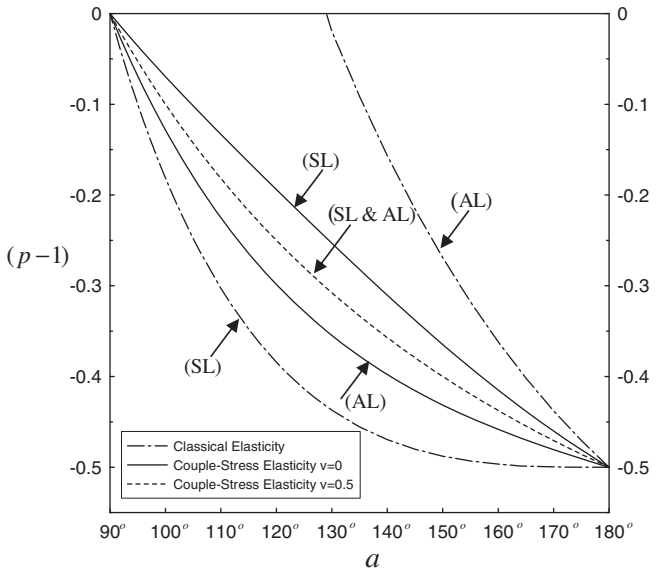

Fig. 4. Variation of the stress singularity with respect to the angle of the notch α for symmetric (SL) and antisymmetric (AL) loadings.

-0.5 to 0, in both symmetric and antisymmetric cases. We recall that in classical elasticity, in the range $128.7° < \alpha < 90°$, the antisymmetric field is not singular (see also Fig. 4). The most singular eigenvalue occurs in the crack problem ($\alpha = 180°$). However, contrary to the classical elasticity case, the singularity associated with the antisymmetric loading is always *stronger* than the respective one in the symmetric loading. Finally, it is noted that the singularity of the stress field depends not only upon the angle of the notch α but also upon the Poisson's ratio ν. In the special case of an incompressible material ($\nu = 0.5$), the variation of the stress singularity is the same for both symmetric and antisymmetric loadings.

The variation of the singularity of the couple-stresses is depicted in Fig. 5. The strength of the singularity depends *only* upon the angle of the notch. It is also seen that in the antisymmetric case the couple-stress field is not singular.

Finally, Fig. 6 shows the variation of the exponent of the dominant part of the rotation. We observe that in couple-stress

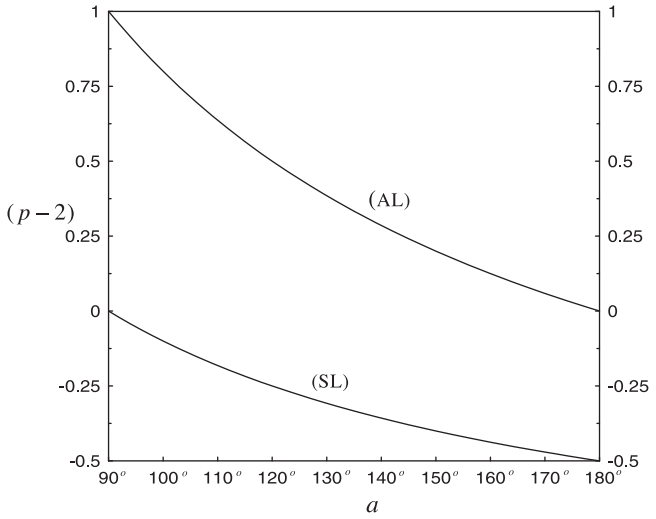

Fig. 5. Variation of the couple-stress singularity with respect to the angle of the notch α for symmetric (SL) and antisymmetric (AL) loadings.

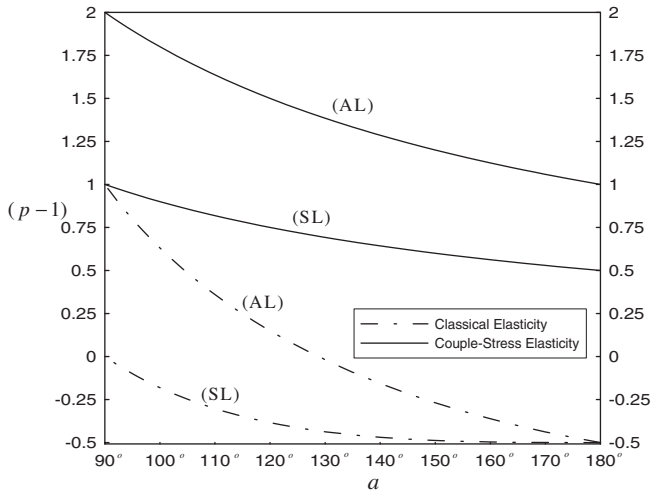

Fig. 6. Variation of the rotation singularity with respect to the angle of the notch a for symmetric (SL) and antisymmetric (AL) loadings.

elasticity the rotation is *bounded* for all notch angles. However, as in classical elasticity, the strain field remains unbounded at the tip of the notch. This can be deduced from Fig. 4, since the dominant part of the strain (41) and stress field (46) varies in the same manner.

The mode I and mode II crack problems are examined now as limit cases of the general notch problem. Plane-strain crack problems were first investigated, in the context of couple-stress elasticity, by Sternberg and Muki (1967), and more recently by Huang et al. (1997, 1999) and Gourgiotis and Georgiadis (2007, 2008). In particular, Huang et al. (1997) using the method of eigenfunction expansions, provided near-tip asymptotic fields for the mode I and mode II crack problems. In their analyses they adopted a direct formulation in terms of stresses and couple-stresses, assuming *a priori* that both fields had the same order of singularity near the crack-tip. However, in the general notch problem the singularities of the stress and couple-stress fields vary differently. Therefore, the displacement formulation employed in the present study is more appropriate.

In the mode I case, the first admissible eigenvalue that defines the singularity of the stress field is $p = 1/2$ (see Fig. 4). The second eigenvalue $p = 1$ produces a constant strain field, while $p = 3/2$ characterizes the singularity of the couple-stress field. In light of the above, the displacement field in (38) takes now the following form

$$u_r = \frac{A_1}{3} r^{1/2}\left[(3-6\nu)\cos\frac{\theta}{2} - (7-6\nu)\cos\frac{3\theta}{2}\right] + 2A_1' r\left[\cos^2\theta - \nu\right] + r^{3/2}\left\{A_1''\left[(5-10\nu)\cos\frac{\theta}{2} - (9-10\nu)\cos\frac{5\theta}{2}\right] + A_3''\left[-\cos\frac{\theta}{2} + 5\cos\frac{5\theta}{2}\right]\right\} + O(r^2), \tag{57a}$$

$$u_\theta = \frac{A_1}{3} r^{1/2}\left[-(1-2\nu)\sin\frac{\theta}{2} + (7-6\nu)\sin\frac{3\theta}{2}\right] - A_1' r\sin 2\theta + r^{3/2}\left\{A_1''\left[-(1-2\nu)\sin\frac{\theta}{2} + (9-10\nu)\sin\frac{5\theta}{2}\right] + 5A_3''\left[\sin\frac{\theta}{2} - \sin\frac{5\theta}{2}\right]\right\} + O(r^2), \tag{57b}$$

where A_1, A_1' and (A_1'', A_3'') are amplitude factors that correspond to the eigenvalues $p = 1/2$, $p = 1$ and $p = 3/2$, respectively.

Further, the stress field becomes

$$\sigma_{rr} = \frac{\mu A_1}{3} r^{-1/2}\left[(3+2\nu)\cos\frac{\theta}{2} - (7-6\nu)\cos\frac{3\theta}{2}\right] + 4\mu A_1' \cos^2\theta + O(r^{1/2}), \tag{58a}$$

$$\sigma_{\theta\theta} = \frac{\mu A_1}{3} r^{-1/2}\left[(5-2\nu)\cos\frac{\theta}{2} + (7-6\nu)\cos\frac{3\theta}{2}\right] + 4\mu A_1' \sin^2\theta + O(r^{1/2}), \tag{58b}$$

$$\sigma_{r\theta} = \frac{\mu A_1}{3} r^{-1/2}\left[-(9-10\nu)\sin\frac{\theta}{2} + (7-6\nu)\sin\frac{3\theta}{2}\right] - 2\mu A_1' \sin 2\theta + O(r^{1/2}), \tag{58c}$$

$$\sigma_{\theta r} = \frac{\mu A_1}{3} r^{-1/2}\left[(7-6\nu)\sin\frac{\theta}{2} + (7-6\nu)\sin\frac{3\theta}{2}\right] - 2\mu A_1' \sin 2\theta + O(r^{1/2}), \tag{58d}$$

where the symmetric and antisymmetric parts of stress are given by

$$\tau_{r\theta} = \tau_{\theta r} = \frac{\mu A_1}{3} r^{-1/2}\left[-(1-2\nu)\sin\frac{\theta}{2} + (7-6\nu)\sin\frac{3\theta}{2}\right] - 2\mu A_1' \sin 2\theta + O(r^{1/2}), \tag{59}$$

$$\alpha_{r\theta} = -\alpha_{\theta r} = -\frac{8\mu(1-\nu)A_1}{3} r^{-1/2}\sin\frac{\theta}{2} + O(r^{1/2}). \tag{60}$$

Moreover, the leading order terms of the rotation and couple stresses assume the form

$$\omega = 6A_3'' r^{1/2}\sin\frac{\theta}{2} + O(r^{3/2}), \tag{61}$$

$$m_{rz} = 12\mu\ell^2 A_3'' r^{-1/2}\sin\frac{\theta}{2} + O(r^{1/2}), \tag{62a}$$

$$m_{\theta z} = 12\mu\ell^2 A_3'' r^{-1/2}\cos\frac{\theta}{2} + O(r^{1/2}). \tag{62b}$$

Turning now to the mode II case, we note that the eigenvalue $p = 1/2$ defines the singularity of the stress field (see Fig. 4). In addition, the second and third consecutive eigenvalues (i.e. $p = 1$, $p = 3/2$) contribute only to the stress field (Fig. 3), while the fourth eigenvalue $p = 2$ characterizes the singularity of the couple-stress field. In this case the displacement field becomes

$$u_r = \frac{B_1}{3} r^{1/2}\left[-(3-6\nu)\sin\frac{\theta}{2} + (5-2\nu)\sin\frac{3\theta}{2}\right] - 2(1-\nu)B_1' r\sin 2\theta + B_1'' r^{3/2}\left[(5-10\nu)\sin\frac{\theta}{2} + (3+2\nu)\sin\frac{5\theta}{2}\right] + O(r^2), \tag{63a}$$

$$u_\theta = \frac{B_1}{3} r^{1/2}\left[-(1-2\nu)\cos\frac{\theta}{2} + (5-2\nu)\cos\frac{3\theta}{2}\right] - 2(1-\nu)B_1' r\cos 2\theta + B_1'' r^{3/2}\left[(1-2\nu)\cos\frac{\theta}{2} + (3+2\nu)\cos\frac{5\theta}{2}\right] + O(r^2), \tag{63b}$$

where B_1, B_1' and B_1'' are amplitude factors that correspond to the eigenvalues $p = 1/2$, $p = 1$ and $p = 3/2$, respectively.

Further, the rotation, stress and couple-stress fields become

$$\omega = \frac{3}{2} B_3''' r\cos\theta + O(r^2), \tag{64}$$

$$\sigma_{rr} = \frac{\mu B_1}{3} r^{-1/2}\left[-(3+2\nu)\sin\frac{\theta}{2} + (5-2\nu)\sin\frac{3\theta}{2}\right] - 4\mu(1-\nu)B_1' \sin 2\theta + O(r^{1/2}), \tag{65a}$$

$$\sigma_{\theta\theta} = -\frac{\mu(5-2\nu)B_1}{3} r^{-1/2}\left[\sin\frac{\theta}{2} + \sin\frac{3\theta}{2}\right] + 4\mu(1-\nu)B_1' \sin 2\theta + O(r^{1/2}), \tag{65b}$$

$$\sigma_{r\theta} = \frac{\mu B_1}{3} r^{-1/2}\left[-(9-10\nu)\cos\frac{\theta}{2} + (5-2\nu)\cos\frac{3\theta}{2}\right] - 8\mu(1-\nu)B_1' \cos^2\theta + O(r^{1/2}), \tag{65c}$$

$$\sigma_{\theta r} = \frac{\mu B_1}{3} r^{-1/2}\left[(7-6\nu)\cos\frac{\theta}{2} + (5-2\nu)\cos\frac{3\theta}{2}\right] + 8\mu(1-\nu)B_1' \sin^2\theta + O(r^{1/2}), \tag{65d}$$

$$\tau_{r\theta} = \tau_{\theta r} = \frac{\mu B_1}{3} r^{-1/2}\left[-(1-2\nu)\cos\frac{\theta}{2} + (5-2\nu)\cos\frac{3\theta}{2}\right] - 4\mu(1-\nu)B_1' \cos 2\theta + O(r^{1/2}), \tag{66}$$

$$\alpha_{r\theta} = -\alpha_{\theta r} = -\frac{8\mu(1-\nu)B_1}{3} r^{-1/2}\cos\frac{\theta}{2} - 4\mu(1-\nu)B_1' + O(r^{1/2}). \tag{67}$$

$$m_{rz} = 6\mu\ell^2 B_3''' \cos\theta + O(r^{1/2}), \tag{68a}$$

$$m_{\theta z} = -6\mu\ell^2 B_3''' \sin\theta + O(r^{1/2}), \tag{68b}$$

where B_3''' is the amplitude factor that corresponds to the eigenvalue $p = 2$.

Regarding now the previous asymptotic results, we note the following points: (i) The stresses exhibit a square-root singularity as in the classical theory of elasticity. However, it is important to observe that while the order of the stress singularities is preserved their detailed structure is altered. Indeed, the singular terms in the stress field, though independent of the characteristic length ℓ, involve the Poisson's ratio ν. (ii) The constant (independent upon the radial distance r) terms in the asymptotic expansion for the stresses (see Eqs. (58) and (65)) correspond to the T-stress field of classical fracture mechanics. However, in contrast with what happens in classical elasticity, where the T-stress field appears only in the mode I crack problem (Anderson, 1995), it is observed here that a constant stress field exists in both plane-strain modes. This is justified from the fact that the $O(r)$ terms (in the asymptotic expansions for the displacements in both mode I and II cases) are coupled, through the boundary conditions with the $O(r^3)$ terms. (iii) The rotation is bounded at the crack-tip vicinity and this concurs with the uniqueness theorem for plane-strain crack problems in couple-stress elasticity (Grentzelou and Georgiadis, 2005). (iv) The couple-stresses exhibit a square-root singularity in the mode I case, whereas in the mode II case the couple-stress field is bounded in the vicinity of the crack-tip. These results are consistent with the behavior of the rotation ω in (61) and (64), respectively. (v) Finally, it should be remarked that the above asymptotic results agree with the ones obtained by Huang et al. (1997).

Next, we consider the special case of a half-space ($\alpha = 90°$). According to Figs. 2 and 3, the first admissible eigenvalue for both symmetric and antisymmetric loadings is $p = 1$. This eigenvalue defines the singularity of the stress field. Further, the eigenvalues $p = 2$ and $p = 3$ determine the singularity of the couple-stress field in the symmetric and the antisymmetric cases, respectively (see also Fig. 5).

In the symmetric case the displacement field takes the following form

$$u_r = A_1 r[(1-2\nu) - \cos 2\theta] + r^2\left\{\frac{A_1'}{3}[(5-6\nu)\cos 3\theta + (3-6\nu)\cos\theta] - \frac{A_3'}{2}(1-3\nu)\cos 3\theta\right\} + O(r^3), \tag{69a}$$

$$u_\theta = A_1 r\sin 2\theta - r^2\left\{\frac{A_1'}{3}[(5-6\nu)\sin 3\theta + (1-2\nu)\sin\theta] - \frac{A_3'}{2}[2(1-2\nu)\sin\theta + (1-3\nu)\sin 3\theta]\right\} + O(r^3), \tag{69b}$$

where A_1, (A_1', A_3') are the amplitude factors that correspond to the eigenvalues $p = 1$ and $p = 2$, respectively.

Further, the rotation, stresses and couple-stresses become

$$\omega = \frac{3}{2}A_3' r\sin\theta + O(r^2), \tag{70}$$

$$\sigma_{\theta\theta} = 2\mu A_1[1 + \cos 2\theta] + O(r), \tag{71a}$$

$$\sigma_{rr} = 2\mu A_1[1 - \cos 2\theta] + O(r), \tag{71b}$$

$$\sigma_{r\theta} = 2\mu A_1 \sin 2\theta + O(r), \tag{71c}$$

$$\sigma_{\theta r} = 2\mu A_1 \sin 2\theta + O(r). \tag{71d}$$

$$\tau_{r\theta} = \tau_{\theta r} = 2\mu A_1 \sin 2\theta + O(r), \tag{72}$$

$$\alpha_{\theta r} = -\alpha_{r\theta} = O(r). \tag{73}$$

$$m_{rz} = 6\mu\ell^2 A_3' \sin\theta + O(r), \tag{74a}$$

$$m_{\theta z} = 6\mu\ell^2 A_3' \cos\theta + O(r). \tag{74b}$$

It is worth noting that the dominant part of the stress tensor is symmetric and coincides with its classical counterpart. Similar results apply for the antisymmetric loading case.

4. Conclusions

In this work, the asymptotic near-tip fields of an elastic plane-strain notch are determined in a solid characterized by the theory of couple-stress elasticity. The boundary value problem was treated with the asymptotic Knein–Williams technique. Our analysis led to an eigenvalue problem, which, along with the restriction of a bounded potential energy, provided the asymptotic fields. The results of the near-tip fields showed departure from the predictions of classical elasticity. In particular, it was found that the dominant displacement field at tip of the notch is always irrotational. In addition, the rotation is bounded for all notch angles, while the strain field remains singular as in the classical theory. The strength of the stress singularity depends not only upon the angle of the notch but also upon the Poisson's ratio ν. Moreover, it varies from $-1/2$ (crack case) to 0 (half-space case) for both symmetric and antisymmetric loadings. Finally, unlike the classical elasticity case, the couple-stress theory predicts that the strength of the singularity associated with the antisymmetric loading is always stronger than the respective one in the symmetric loading. This finding corroborates the fact that shear effects are more pronounced when couple-stresses are taken into account (Huang et al., 1999; Gourgiotis and Georgiadis, 2007, 2008).

Acknowledgement

The research leading to these results has received funding from the European Research Council under the European Community's

Seventh Framework Programme (FP7/2007-2013)/ERC grant agreement no. 228051.

Appendix A. Derivation of the higher-order terms in the near-tip asymptotic expansion

Substituting Eq. (36) in the field Eqs. (34), and equating coefficients of like powers of r, we obtain the following non-homogeneous system of coupled ordinary differential equations for the angular functions $U_1(\theta)$ and $V_1(\theta)$:

$$\begin{cases} \ell^2(1-2\nu)\Big[U_1^{iv}+2(p^2+2p-1)U_1''+(p+1)^2(p+3)(p-1)U_1 \\ \quad -4V_1'''-4(p+1)^2V_1'\Big]-(1-2\nu)U_0''-(p+4\nu-3)V_0'-2(1-\nu)(p^2-1)U_0=0 \\ \ell^2(1-2\nu)\Big[V_1^{iv}+2(p^2+2p-1)V_1''+(p+1)^2(p+3)(p-1)V_1 \\ \quad +4U_1'''+4(p+1)^2U_1'\Big]-2(1-\nu)V_0''-(p-4\nu+3)U_0'-(1-2\nu)(p^2-1)V_0=0, \end{cases} \tag{A1}$$

where $U_0(\theta)$ and $V_0(\theta)$ are defined in Eqs. (38).

The general solution of the system (A1) is

$$\begin{aligned} U_1(\theta) = {} & \left\{ \frac{1}{(1-2\nu)\ell^2}\left[\frac{(1-\nu)}{2(p+1)}A_1+\frac{(p-3+4\nu)}{16p}A_3\right]\cos(p-1)\theta \right. \\ & +\frac{1}{48}A_4\frac{(p-12\nu+9)}{(1-2\nu)\ell^2 p}\cos(p-3)\theta+C_1\cos(p+1)\theta \\ & \left. -C_2\cos(p+3)\theta+C_4\cos(p-1)\theta\right\} \\ & +\left\{ \frac{1}{(1-2\nu)\ell^2}\left[\frac{(1-\nu)}{2(p+1)}B_1-\frac{(p-3+4\nu)}{16p}B_3\right]\sin(p-1)\theta \right. \\ & +\frac{1}{48}B_4\frac{(p-12\nu+9)}{(1-2\nu)\ell^2 p}\sin(p-3)\theta+D_1\sin(p+1)\theta \\ & \left. +D_2\sin(p+3)\theta-D_4\sin(p-1)\theta\right\}, \end{aligned} \tag{A2a}$$

$$\begin{aligned} V_1(\theta) = {} & \left\{ -\frac{1}{48}A_4\frac{(p+12\nu-9)}{(1-2\nu)\ell^2 p}\sin(p-3)\theta+C_2\sin(p+3)\theta \right. \\ & \left. +C_3\sin(p+1)\theta+C_4\sin(p-1)\theta\right\} \\ & +\left\{ \frac{1}{48}B_4\frac{(p+12\nu-9)}{(1-2\nu)\ell^2 p}\cos(p-3)\theta+D_2\cos(p+3)\theta \right. \\ & \left. +D_3\cos(p+1)\theta+D_4\cos(p-1)\theta\right\}. \end{aligned} \tag{A2b}$$

Moreover, the displacement field should also satisfy Eq. (33) (i.e. $\nabla^2 e = 0$). Accordingly, we obtain the following uncoupled differential equations for the angular functions $(U_0(\theta),\ V_0(\theta))$ and $(U_1(\theta), V_1(\theta))$

$$V_0'''(\theta)+(p-1)^2V_0'(\theta)+(p+1)U_0''(\theta)+(p-1)^2(p+1)U_0(\theta)=0, \tag{A3}$$

$$V_2'''(\theta)+(p+1)^2V_2'(\theta)+(p+3)U_2''(\theta)+(p+1)^2(p+3)U_2(\theta)=0. \tag{A4}$$

Substituting Eqs. (A2) into (A3) and (A4), we get the following relations between the amplitudes:

$$A_4=B_4=0 \tag{A5}$$

and

$$\begin{aligned} C_4 &= -\frac{(p+3)}{4(p+1)\ell^2(1-2\nu)}\left[\frac{(1-\nu)}{(p+1)}A_1+\frac{(p+4\nu-3)}{8p}A_3\right], \\ D_4 &= \frac{(p+3)}{4(p+1)\ell^2(1-2\nu)}\left[\frac{(1-\nu)}{(p+1)}B_1-\frac{(p+4\nu-3)}{8p}B_3\right]. \end{aligned} \tag{A6}$$

Incorporating the above results we finally obtain Eqs. (39) and (40) for the displacement field.

References

Aero, E.L., Kuvshinskii, E.V., 1960. Fundamental equations of the theory of elastic media with rotationally interacting particles. Fizika Tverdogo Tela 2, 1272–1281 (Translated in Soviet Physics-Solid State 2 (1961) 1399–1409).

Anderson, T.L., 1995. Fracture Mechanics: Fundamentals and Applications. CRC Press, Boca Raton, FL.

Atkinson, C., Leppington, F.G., 1977. The effect of couple stresses on the tip of a crack. International Journal of Solids and Structures 13, 1103–1122.

Barber, J.R., 1992. Elasticity. Kluwer Academic Publishers, Dordrecht.

Bardet, J.P., Vardoulakis, I., 2001. The asymmetry of stress in granular media. International Journal of Solids and Structures 38, 353–367.

Bigoni, D., Drugan, W.J., 2007. Analytical derivation of Cosserat moduli via homogenization of heterogeneous elastic materials. ASME Journal of Applied Mechanics 74, 741–753.

Bogy, D.B., Sternberg, E., 1967. The effect of couple-stresses on singularities due to discontinuous loadings. International Journal of Solids and Structures 3, 757–770.

Bogy, D.B., Sternberg, E., 1968. The effect of couple-stresses on the corner singularity due to an asymmetric shear loading. International Journal of Solids and Structures 4, 159–174.

Brahtz, J.H.A., 1933. Stress distribution in a reentrant corner. Transactions of ASME Series E 55, 31–37.

Chang, C.S., Shi, Q., Liao, C.L., 2003. Elastic constants for granular materials modeled as first-order strain-gradient continua. International Journal of Solids and Structures 40, 5565–5582.

Chen, J.Y., Huang, Y., Ortiz, M., 1998. Fracture analysis of cellular materials: a strain gradient Model. Journal of the Mechanics and Physics of Solids 46, 789–828.

Cosserat, E., Cosserat, F., 1909. Theorie des Corps Deformables. Hermann et Fils, Paris.

Dundurs, J., Markenscoff, X., 1989. Sternberg-Koiter conclusion and other anomalies of the concentrated couple. ASME Journal of Applied Mechanics 56, 240–245.

Ejike, U.B.C.O., 1969. The plane circular crack problem in the linearized couple-stress theory. International Journal of Engineering Science 7, 947–961.

Fleck, N.A., Muller, G.M., Ashby, M.F., Hutchinson, J.W., 1994. Strain gradient plasticity: theory and experiment. Acta Metallurgica et Materialia 42, 475–487.

Georgiadis, H.G., Velgaki, E.G., 2003. High-frequency Rayleigh waves in materials with microstructure and couple-stress effects. International Journal of Solids and Structures 40, 2501–2520.

Gourgiotis, P.A., Georgiadis, H.G., 2007. Distributed dislocation approach for cracks in couple-stress elasticity: shear modes. International Journal of Fracture 147, 83–102.

Gourgiotis, P.A., Georgiadis, H.G., 2008. An approach based on distributed dislocations and disclinations for crack problems in couple-stress elasticity. International Journal of Solids and Structures 45, 5521–5539.

Gourgiotis, P.A., Sifnaiou, M.D., Georgiadis, H.G., 2010. The problem of sharp notch in microstructured solids governed by dipolar gradient elasticity. International Journal of Fracture 166, 179–201.

Gregory, R.D., 1979. Green's functions, bi-linear forms, and completeness of the eigenfunctions for the elastostatic strip and wedge. Journal of Elasticity 9, 283–309.

Grentzelou, C.G., Georgiadis, H.G., 2005. Uniqueness for plane crack problems in dipolar gradient elasticity and in couple-stress elasticity. International Journal of Solids and Structures 42, 6226–6244.

Harrington, W.J., Ting, T.W., 1971. Stress boundary-value problems for infinite wedges. Journal of Elasticity 1, 65–81.

Hsu, Y.C., Ju, F.D., Wang, W.J., 1972. A couple-stresses elastic solution of an infinite tension plate bounded by an elliptical hole. Journal of Mathematical Analysis and Applications 40, 708–722.

Huang, Y., Zhang, L., Guo, T.F., Hwang, K.C., 1997. Mixed mode near tip fields for cracks in materials with strain-gradient effects. Journal of the Mechanics and Physics of Solids 45, 439–465.

Huang, Y., Chen, J.Y., Guo, T.F., Zhang, L., Hwang, K.C., 1999. Analytic and numerical studies on mode I and mode II fracture in elastic-plastic materials with strain gradient effects. International Journal of Fracture 100, 1–27.

Itou, S., 1976. The effect of couple-stresses on stress concentrations around a circular hole in a strip under tension. International Journal of Engineering Science 14, 861–867.

Jaunzemis, W., 1967. Continuum Mechanics. McMillan, New York.

Karp, S.N., Karal, F.C., 1962. The elastic-field behavior in the neighborhood of a crack of arbitrary angle. Communications on Pure and Applied Mathematics 15, 413–421.

Knein, M., 1927. Zur Theorie des Druckversuchs. Abhandlungen aus dem aerodynamnischen Institut an der Technischen Hochschule Aachen, Heft 7, 43–62.

Koiter, W.T., 1964. Couple-stresses in the theory of elasticity. Part I, II. Proceedings of the Koninklijke Nederlandse Akademie van Wetenschappen B67, 17–44.
Lakes, R.S., 1983. Size effects and micromechanics of a porous solid. Journal of the Materials Science 18, 2572–2580.
Lakes, R.S., 1993. Strongly Cosserat elastic lattice and foam materials for enhanced toughness. Cellular Polymers 12, 17–30.
Lakes, L., 1995. Experimental methods for study of Cosserat elastic solids and other generalized elastic continua. In: Muhlhaus, H.-B. (Ed.), Continuum Models for Materials with Microstructure. John Wiley and Sons, Chichester, pp. 1–25.
Leguillon, D., 1988. Sur le moment ponctuel appliqué a un secteur: le paradoxe de Sternberg–Koiter. Comptes rendus de l'Académie des Sciences, series II 307, 1741–1746.
Lubarda, V.A., 2003. Circular inclusions in anti-plane strain couple stress elasticity. International Journal of Solids and Structures 40, 3827–3851.
Lubarda, V.A., Markenskoff, X., 2000. Conservation integrals in couple stress elasticity. Journal of the Mechanics and Physics of Solids 48, 553–564.
Maranganti, R., Sharma, P., 2007. A novel atomistic approach to determine strain-gradient elasticity constants: Tabulation and comparison for various metals, semiconductors, silica, polymers and the (ir) relevance for nanotechnologies. Journal of the Mechanics and Physics of Solids 55, 1823–1852.
Mindlin, R.D., 1963. Influence of couple-stresses on stress concentrations. Experimental Mechanics 3, 1–7.
Mindlin, R.D., Tiersten, H.F., 1962. Effects of couple-stresses in linear elasticity. Archive for Rational Mechanics and Analysis 11, 415–448.
Muki, R., Sternberg, E., 1965. The influence of couple-stresses on singular stress concentrations in elastic solids. Journal of Applied Mathematics and Physics (ZAMP) 16, 611–618.
Neuber, H., 1963. Losüng des Carothers-problems mittels prinzipien der kraftübertragung (Keil mit moment an der spitze). Journal of Applied Mathematics and Mechanics (ZAMM) 43, 211–228.
Nowacki, W., 1972. Theory of Micropolar Elasticity. CISM International Centre for Mechanical Sciences, vol. 25. Springer-Verlag.
Palmov, V.A., 1964. The plane problem of non-symmetrical theory of elasticity. Applied Mathematics and Mechanics (PMM) 28, 1117–1120.
Radi, E., 2007. Effects of characteristic material lengths on mode III crack propagation in couple stress elastic-plastic materials. International Journal of Plasticity 23, 1439–1456.
Radi, E., 2008. On the effects of characteristic lengths in bending and torsion on Mode III crack in couple stress elasticity. International Journal of Solids and Structures 45, 3033–3058.
Sinclair, G.B., 2004. Stress singularities in classical elasticity. II: Asymptotic identification. Applied Mechanics Reviews 57, 385–439.
Sternberg, E., Koiter, W.T., 1958. The wedge under concentrated couple: a paradox in the two dimensional theory of elasticity. ASME Journal of Applied Mechanics 26, 472–474.
Sternberg, E., Muki, R., 1967. The effect of couple-stresses on the stress concentration around a crack. International Journal of Solids and Structures 3, 69–95.
Suwito, W., Dunn, M.L., Cunningham, S.J., Read, D.T., 1999. Elastic moduli, strength, and fracture initiation at sharp notches in etched single crystal silicon microstructures. Journal of Applied Physics 85, 3519–3534.
Takeuti, Y., Noda, N., 1973. Thermal stresses and couple-stresses in square cylinder with a circular hole. International Journal of Engineering Science 11, 519–530.
Toupin, R.A., 1962. Perfectly elastic materials with couple stresses. Archive for Rational Mechanics and Analysis 11, 385–414.
Vardoulakis, I., Sulem, J., 1995. Bifurcation Analysis in Geomechanics. Blackie Academic and Professional (Chapman and Hall), London.
Voigt, W., 1887. Theoritiscke Studien uber die Elastizitatsverhaltnisse der Krystalle. Abhandlungen der Königlichen Gesellschaft der Wissenschaften zu Göttingen 34, 3–51.
Weitsman, Y., 1965. Couple-stress effects on stress concentration around a cylindrical inclusion in a field of uniaxial tension. ASME Journal of Applied Mechanics 32, 424–428.
Williams, M.L., 1952. Stress singularities resulting from various boundary conditions in angular corners of plates in extension. ASME Journal of Applied Mechanics 74, 526–528.
Zhang, L., Huang, Y., Chen, J.Y., Hwang, K.C., 1998. The mode-III full-field solution in elastic materials with strain gradient effects. International Journal of Fracture 92, 325–348.